

Full-stack Comparison of Channel Models for Networks Above 100 GHz in an Indoor Scenario

Amir Ashtari Gargari
Department of
Information Engineering
University of Padova
Padova, Italy
amirashitari@dei.unipd.it

Michele Polese
Institute for the Wireless
Internet of Things
Northeastern University
Boston, MA, USA
m.polese@northeastern.edu

Michele Zorzi
Department of
Information Engineering
University of Padova
Padova, Italy
zorzi@dei.unipd.it

ABSTRACT

The Sixth Generation (6G) of mobile networks is expected to use carrier frequencies in the spectrum above 100 GHz, to satisfy the demands for higher data rates and bandwidth of future digital applications. The development of networking solutions at such high frequencies is challenged by the harsh propagation environment, and by the need for directional communications and signal processing at high data rates. A fundamental step in defining and developing wireless networks above 100 GHz is given by an accurate performance evaluation. For simulations, this strongly depends on the accuracy of the modeling of the channel and of the interaction with the higher layers of the stack. This paper introduces the implementation of two recently proposed channel models (based on ray tracing and on a fully stochastic model) for the 140 GHz band for the ns-3 TeraSim module, which enables simulation of macro wireless networks in the sub-terahertz and terahertz spectrum. We also compare the two channel models with full-stack simulations in an indoor scenario, highlighting differences and similarities in how they interact with the protocol stack and antenna model of TeraSim.

CCS CONCEPTS

• **Networks** → **Network performance evaluation; Mobile networks.**

KEYWORDS

Terahertz, Cellular Networks, mmWave, channel modeling.

ACM Reference Format:

Amir Ashtari Gargari, Michele Polese, Michele Zorzi. 2022. Full-stack Comparison of Channel Models for Networks Above 100 GHz in an Indoor Scenario. In *5th ACM Workshop on Millimeter-Wave and Terahertz Networks and Sensing Systems (mmNets '21)*, January 31–February 4, 2022, New Orleans, LA, USA. ACM, New York, NY, USA, 6 pages. <https://doi.org/10.1145/3477081.3481677>

Permission to make digital or hard copies of all or part of this work for personal or classroom use is granted without fee provided that copies are not made or distributed for profit or commercial advantage and that copies bear this notice and the full citation on the first page. Copyrights for components of this work owned by others than the author(s) must be honored. Abstracting with credit is permitted. To copy otherwise, or republish, to post on servers or to redistribute to lists, requires prior specific permission and/or a fee. Request permissions from permissions@acm.org.
mmNets '21, January 31–February 4, 2022, New Orleans, LA, USA
© 2022 Copyright held by the owner/author(s). Publication rights licensed to ACM.
ACM ISBN 978-1-4503-8699-9/22/01...\$15.00
<https://doi.org/10.1145/3477081.3481677>

1 INTRODUCTION

The society and the economy are becoming more and more reliant on wireless connectivity as the backbone for digital services. Mobile connected devices enable human-to-human communications, remote machine monitoring, control, actuation, as part of the Industry 4.0 paradigm, improve autonomous driving through high-speed data exchange, and empower remote health solutions [7]. As the number of services and users of the wireless spectrum increases, so does the need for increased bandwidth and higher data rates. The 5th Generation (5G) of mobile networks features the first 3rd Generation Partnership Project (3GPP) mobile Radio Access Network (RAN) (i.e., 3GPP NR) to support frequencies in the lower millimeter wave (mmWave) range, i.e., below 52.6 GHz, with extensions to 71 GHz being considered for future 3GPP releases [1, 2].

Nowadays, 5G is being commercially deployed, and the research and industrial community have shifted their focus toward the development of Sixth Generation (6G) solutions [7]. 6G networks will support carrier frequencies in the spectrum above 100 GHz, in the lower part of the terahertz bands, to fulfill the quest for additional bandwidth [3]. For instance, the IEEE 802.15.3d standard has been developed to operate in sub-terahertz frequency bands with up to 69 GHz of bandwidth, to support new applications such as Virtual Reality (VR) and telepresence through 3D holograms [7, 18]. Notably, the spectrum available above 100 GHz is expected to enable terabit-per-second links, which could be also used for high-capacity backhaul, and to facilitate the integration of new paradigms in communications and sensing [22].

The support of carriers at such high frequencies, however, comes with several challenges. For example, the propagation environment is challenging, with a high pathloss, which increases proportionally with the square of the carrier frequency, as the size of an antenna element decreases, and with additional molecular absorption in specific frequency bands. Furthermore, communications in the mmWave and terahertz spectrum are affected by blockage, as signals do not penetrate common materials. From a networking perspective, directionality is key to improving the link budget, but requires the two endpoints of a link to coordinate to identify the best directions to communicate with each other. These issues, together with the challenging data processing at high rates, propagate throughout the whole protocol stack [20].

The development of solutions, algorithms, and protocols for wireless networks above 100 GHz necessitates tools for accurate and reliable performance evaluation. At the time of writing, wireless testbeds for such frequency bands are extremely expensive, due to the need for custom Radio Frequency (RF) components. They are

Channel Model	Frequency	Modeling approach	LOS/NLOS	Characteristics
TeraSim [10]	0.1-10 THz	Physics-based	LOS propagation	Frequency-selective model for propagation at terahertz
FS Channel [12]	28 GHz, 140 GHz	SCM, measurement-based	LOS/NLOS, fading	Stochastic model, scales to randomly generated scenarios for large scale evaluations
HB Channel [5]	130-143 GHz	SCM based on RT and random components, measurement-based	LOS/NLOS, fading	The baseline model is given by RT, accurate in specific, deterministic scenarios.

Table 1: Channel models for above 100 GHz wireless networks considered in this paper.

thus limited to few nodes [23], and mostly focused on physical layer evaluations or channel sounding. In this context, simulations can be used to provide an end-to-end, full-stack performance evaluation platform. This has helped, for example, highlight a number of issues that arise from the interaction between the higher layers of the protocol stack, such as TCP, and the large bandwidth, the blockage phenomena, and the directional communications typical of these frequency bands [20, 25]. The accuracy of simulations, however, strongly depends on the accuracy of the channel model, and on how it is possible to represent its interactions with the rest of the device and protocol stack components (e.g., the directional antenna components), as also discussed in [14].

Recent papers have proposed measurement-based channel models for the spectrum above 100 GHz [5, 12, 15], but they have not been considered in the context of an end-to-end, full-stack deployment. Other work has focused on the development of simulation tools for terahertz frequencies, but with a Line of Sight (LOS) channel model [10]. This paper combines both, enabling a full-stack evaluation of wireless networks above 100 GHz with realistic channel models, which include Non Line of Sight (NLOS) and fading modeling.

Notably, the contributions are twofold. First, we review channel modeling options for the spectrum above 100 GHz, and present the implementation for the ns-3 module TeraSim of two Spatial Channel Models (SCMs). The first is the Fully Stochastic (FS) SCM introduced in [12], while the second is a Hybrid (HB) channel model introduced in [5], which combines ray tracing with additional stochastic components. We selected these channel modeling strategies for implementation and comparison as they present a trade-off between generality and accuracy. Fully stochastic models can be applied in generic scenarios, but are not as precise as RT-based channels when considering specific deployments. Conversely, RT-based channels have a higher computational overhead, as they require the generation of Multi-path Components (MPCs) using an RT. Additionally, SCMs can be used for performance evaluation with antenna arrays and directional communications.

The second contribution is a full-stack comparison of the two channel modeling strategies in an indoor office scenario. We investigate the interplay between the antenna and the channel modeling using UDP as transport protocol, and different source traffic configurations. Our results show that different channel models (with different spatial distribution of the MPCs) have a different interplay with directional antenna models, which eventually result into different full-stack throughput and latency values. These results can inform the design of simulation campaigns for evaluation of

future 6G networks in generic and/or specific scenarios. Finally, we open source the channel modeling code as additional contribution to the community.¹

The rest of the paper is organized as follows. Section 2 introduces and qualitatively compares the two channel models. Section 3 discusses the implementation for the ns-3 TeraSim module, and Section 4 presents the results for the numerical comparison between the channel models. Finally, Section 5 concludes the paper.

2 CHANNEL MODELING ABOVE 100 GHZ

The development of 5G networks in the lower mmWave band has been initially driven by the identification of channel models, such as those discussed in [6, 21]. Similarly, the focus of channel modeling in above 100 GHz bands is shifting from the analysis of the propagation and molecular absorption [11] to SCM models [8, 9, 16, 17]. These are useful for evaluations with antenna arrays, and include fading and LOS/NLOS characterizations. Recent examples are the models published in [5, 12, 15]. Table 1 summarizes the common characteristics and differences between the different modeling approaches considered in this paper, which we selected as representative of fully stochastic and RT-based models, as discussed in Section 1. In the next paragraphs, we will discuss in detail the FS and HB models, which will then be compared in Sec. 4.

2.1 Hybrid Channel Modeling

The HB model [5] characterizes indoor sub-terahertz propagation by combining RT techniques and stochastic methods. This channel model is built upon wideband channel measurements conducted at 130–143 GHz frequencies in a standard conference room. The HB model comprises MPC clustering and matching procedures with RT techniques to study the cluster behavior and wave propagation in the terahertz spectrum [4]. The RT component makes it possible to accurately account for realistic scattering conditions in a specific scenario, while the stochastic element models random scatterers (e.g., wall texture, or small objects) that may be difficult to properly capture within the RT scenario [13]. The Channel Impulse Response (CIR) as a function of the frequency f is given by

$$h_{HB}(\tau, \theta, f) = h_{RT}(\tau, \theta, f) + h_S(\tau, \theta, f), \quad (1)$$

where τ and θ indicate the delay and azimuth Angle of Arrival (AoA), and $h_{RT}(\cdot)$ and $h_S(\cdot)$ are the channel components modeled through RT and stochastic methods. h_{RT} combines the Fresnel equations with the geometrical data to estimate the LOS and the reflection losses from the scattering of the walls (central sub-path

¹The code is available at <https://github.com/signetlabdei/thz-mmnets-2021>.

in RT clusters). Conversely, h_S models stochastically the diffraction of other sub-paths in the RT clusters, and the scattering of the reflections from additional obstacles (non-RT clusters). The CIR generated by the RT, $h_{RT}(\tau, \theta, f)$, is represented as

$$h_{RT}(\tau, \theta, f) = A_t(\phi_{LoS})\alpha_{LoS}(f)\delta(\tau - \tau_{LoS})\delta(\theta - \theta_{LoS}) + \sum_{l=1}^{L_{RT}} A_t(\phi_{l,0})\alpha_{l,0}(f)\delta(\tau - \tau_{l,0})\delta(\theta - \theta_{l,0}), \quad (2)$$

where the subscript $l, 0$ indicates the central path in the l^{th} sub-path, $A_t(\cdot)$ represents the antenna pattern at the Transmitter (TX), and $\alpha_{l,0}$, $\tau_{l,0}$, $\theta_{l,0}$ and $\phi_{l,0}$ represent amplitude gain, Time of Arrival (ToA), azimuth AoA, and Angle of Departure (AoD) vectors of the sub-path, respectively. L_{RT} is the number of RT clusters. The CIR of the stochastic component, $h_S(\tau, \theta, f)$, is represented as

$$h_S(\tau, \theta, f) = \sum_{l=1}^{L_{RT}} \sum_{p=-Q_l, p \neq 0}^{P_l} A_t(\phi_{l,p})\alpha_{l,p}(f)\delta(\tau - \tau_{l,p})\delta(\theta - \theta_{l,p}) + \sum_{q=1}^{L_s} \sum_{s=-T_q}^{S_q} \alpha_{q,s}(f)\delta(\tau - \tau_{q,s})\delta(\theta - \theta_{q,s}), \quad (3)$$

where subscripts l, p and s, q indicates the p^{th} sub-path in the l^{th} RT cluster, and the s^{th} sub-path in the q^{th} non-RT cluster, respectively. Notice that the antenna pattern of the TX is not involved in the statistical CIR in (3). The reason is that all statistical parameters are extracted from channel measurements with the directional antenna TX, so the effect of the antenna is contained in the generated amplitude.

2.2 Fully Stochastic Modeling

The FS channel model [12] is a 3GPP-like indoor spatial SCM. This model is based on an experimental channel measurement campaign at 28 GHz and 140 GHz, in an office environment. The channel model is based on the concept of Time Cluster (TC) and Spatial Lobe (SL), which represent temporal and spatial statistics of the channel model, respectively. TCs comprise MPCs propagating adjacent in time, which may come from different AoA (AoD), whereas SLs define the main direction of arrival (departure). The directional CIR is

$$h_{FS}(\tau, \phi, \theta) = \sum_{n=1}^N \sum_{m=1}^{M_n} a_{n,m} e^{j\varphi_{n,m}} \delta(\tau - \tau_{n,m}) g_{TX}(\phi - \phi_{n,m}) g_{RX}(\theta - \theta_{n,m}), \quad (4)$$

where τ , ϕ , and θ are the absolute propagation delay, AoD vector, and AoA vector, respectively. Also, g_{TX} and g_{RX} are the TX and Receiver (RX) complex amplitude antenna patterns, respectively.

3 INTEGRATION IN TERASIM

Network Simulator 3 (ns-3) is a discrete-event network simulation environment, which models a wide range of wireless and wired technologies, as well as the TCP/IP protocol stack and applications. TeraSim [10] is an extension of ns-3 for the modeling of Terahertz (THz) communication networks. The TeraSim module enables simulation-based testing of THz networking protocols in

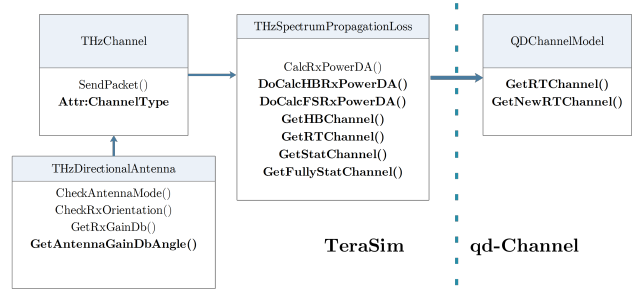


Figure 1: TeraSim classes and new channel modeling code.

the higher layers without dealing with lower layer configurations. In the following paragraphs we will briefly describe the TeraSim module, and then discuss the integration of the channel models from Sec. 2.

3.1 ns-3 TeraSim Module

TeraSim is the first simulation platform for THz communication networks that supports THz devices' capabilities, from the protocol stack to the modeling of directional antenna patterns [24]. TeraSim considers two types of application scenarios, i.e., nano-scale scenarios, for short-range communications, and macro-scale, for traditional macro (e.g., cellular) scenarios. The module features common channel, antenna, and energy models for nano and macro applications, and separate Medium Access Control (MAC) and Physical (PHY) models.

The antenna model of TeraSim is based on the directional communication scheme introduced in [24], where alignment between mobile nodes is achieved with a rotating antenna. The model is implemented in the *THzDirectionalAntenna* class, which extends the ns-3 cosine antenna with the possibility to rotate. The *THzDirectionalAntenna* class calculates the antenna gain based on the mobility and the RX orientation. It is possible to configure different parameters for the antenna model, including whether the antenna is static or rotates, the rotation speed and initial phase, the maximum gain and beamwidth. A beamwidth of 360 degrees models an omnidirectional antenna.

The already implemented channel model (based on [11]) accounts for the frequency selectivity based on different molecular absorption patterns at different frequencies of the terahertz spectrum. However, the current implementation of TeraSim only accounts for LOS propagation. As the evaluation of network performance in NLOS conditions is key for a holistic evaluation of the performance of future 6G networks, we describe below the implementation of two channel models that also account for NLOS propagation.

3.2 Integration of HB and FS Channels

TeraSim models the waveform propagation through the wireless channel in the *THzChannel* class, as shown in Figure 1. The *THzSpectrumValueFactory* class generates an object representing a waveform and passes it to the channel object. This first checks the orientation of the devices, and obtains the antenna gains through

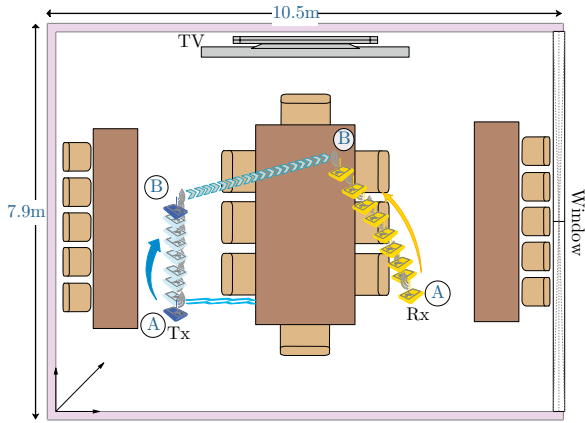


Figure 2: Simulation scenario. The TX and RX move from point A to point B.

the *THzDirectionalAntenna* module. Then, the *THzSpectrumPropagationLoss* class calculates the received power based on the calculated antenna gain and the CIR. The CIR is frequency selective and a function of the distance and frequency. Finally, the *THzChannel* object passes the packet along with the received power to the physical layer of receivers.

Figure 1 summarizes the integration that we have made to support the HB and FS in TeraSim. Most of the updates have been introduced in the *THzSpectrumPropagationLoss* class. Two new functions are responsible for calculating the received power for HB and FS channels, and the type of channel can be selected through the *ChannelType* attribute in the *THzChannel* class. Additionally, while the CIR for FS is generated at run-time in ns-3, the CIR for the HB requires the generation of the RT MPCs offline. For this, we use the Q-D Channel RT tool [13, 14], an open-source MATLAB-based RT tool for the mmWave spectrum. We updated the parameters (e.g., permittivity) in the material library and the path loss equation with those introduced in [5, 19]. The MPCs generated by the RT are then loaded at run-time using the ns-3 qd-channel module.²

²<https://github.com/signetlabdei/qd-channel>

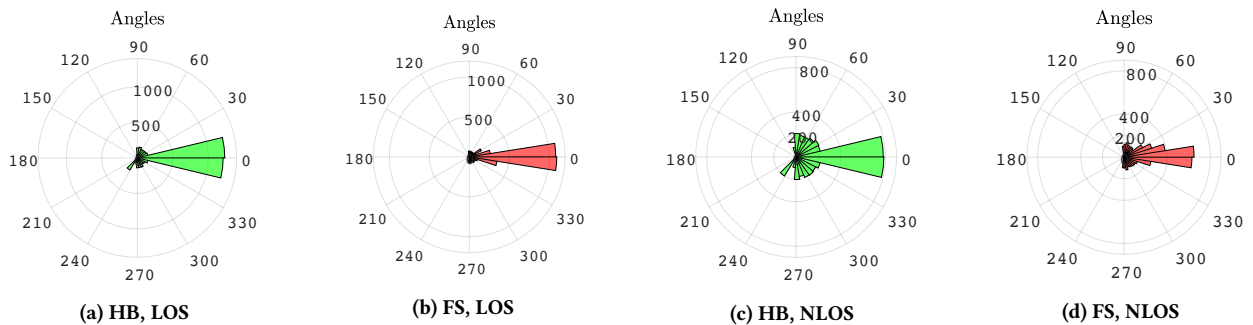


Figure 4: AoA distribution over 2000 channel realizations, for the HB and FS models, in LOS and NLOS. The LOS direction corresponds to 0 degrees.

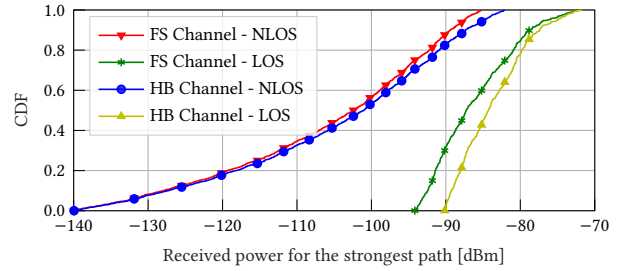


Figure 3: Cumulative Distribution Function (CDF) of the received power (including the antenna gain) for the strongest path, beamwidth 8 degrees

4 PERFORMANCE EVALUATION

This section introduces a performance evaluation in an indoor scenario (Sec. 4.1), with a comparison between the results that can be obtained with the HB and the FS channel models (Sec. 4.2).

4.1 Simulation Scenario

As shown in Figure 2, simulations are set in an indoor meeting room, which has the same size as that used for channel measurements in [5]. We consider a mobility pattern for the TX and the RX (from point A to point B in the figure) that covers NLOS and LOS conditions. The carrier frequency for the simulations is 140 GHz, with a bandwidth of 32 GHz. The TX and RX maximum antenna gain is 25 dBi. The Half Power Beamwidth (HPBW) of the RX antenna varies from 2 to 10 degrees, and the noise floor is -160 dBm. The application is a constant bitrate source, with source rates between 4 Gbit/s and 60 Gbit/s, and UDP as transport.

4.2 Results

Two sets of simulations are run to evaluate the performance of HB and FS channels based on the strongest received path. Figure 3 shows the CDF of the received power (including the antenna gain) for the strongest path of HB and FS channels for LOS and NLOS scenarios. As can be seen, the HB model accounts for MPCs with a higher received power in LOS, with an offset smaller than 5 dB. The two channels are similar in NLOS, even though HB slightly outperforms the FS in the third quartile. The spatial profile of the two channels is compared in Figure 4, which shows the distribution

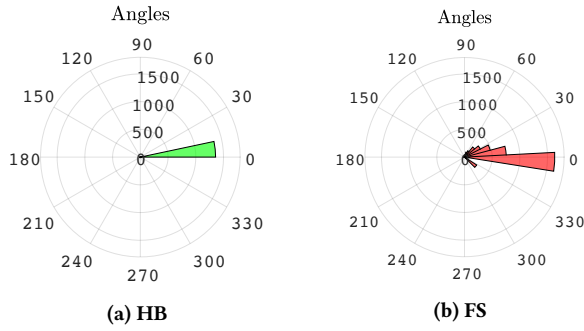


Figure 5: Distribution of the AoA associated with the MPC with highest received power, NLOS

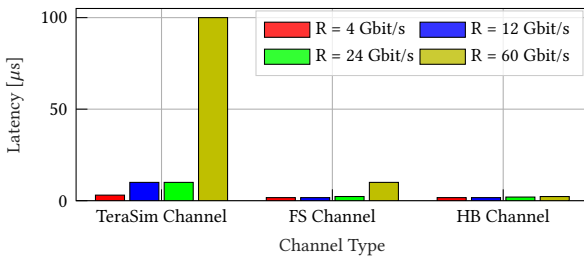


Figure 6: UDP latency with different channel models.

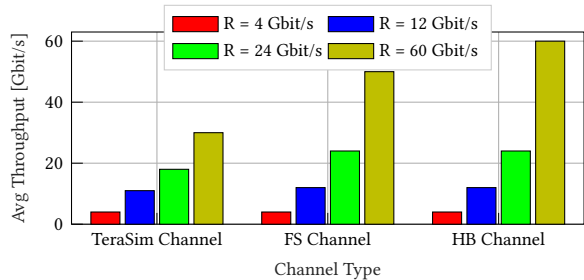


Figure 7: UDP throughput with different channel models.

of the AoA for the MPC for both LOS and NLOS. As expected, the LOS channels are associated to fewer reflected MPCs. Reflections play a minor (but more prominent) role also in the NLOS channels, where the direct path (even though attenuated by the presence of obstacles) is still the most common. This is shown also in Figure 5, which reports the distribution of the MPC corresponding to the strongest path. In general, the HB channel models more MPCs in the direction corresponding to LOS than FS. This, as will be discussed later, has an impact when directional communications with extremely narrow beams are considered.

Figures 6 and 7 compare the latency and throughput, respectively, with the default TeraSim channel model (LOS only), and the HB and FS channels with different source rate values. For the smaller source rate values, the performance with the three channel models is similar, with a slightly higher latency with the TeraSim channel. Indeed, as the bandwidth is underutilized, more robust Modulation

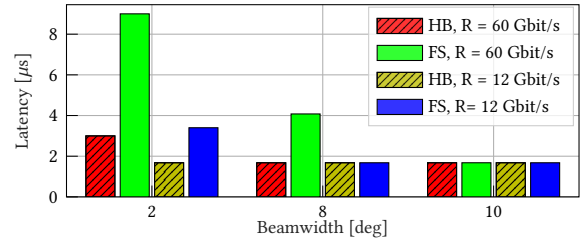


Figure 8: UDP latency for different RX beamwidth.

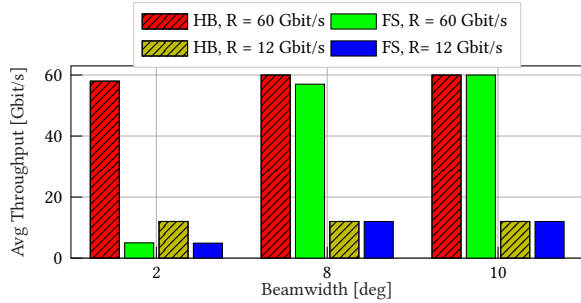


Figure 9: UDP throughput for different RX beamwidth.

and Coding Schemes (MCSs) and buffering can compensate for a weaker channel or a suboptimal coordination among the nodes for directional communications. When the source rate increases to 60 Gbit/s, the difference in the performance measured with the three models increases, with the HB model associated to a higher throughput, and, consequently, lower latency. Notably, a throughput comparable with the full source rate can be achieved only in simulations based on the HB model. This can be explained by analyzing the interaction between the rotating directional antenna model (described in Sec. 3) and the MPC AoA distribution. The HB channel has a higher probability of having the strongest NLOS MPC given by the attenuated component in the LOS direction, thus it is less likely to require adaptation of the antenna direction at the TX and RX. This results into a higher received power than with FS, and thus a higher throughput.

This consideration extends to the results shown in Figures 8 and 9, which report the latency and throughput for different values of the RX antenna beamwidth and the HB and FS channels. Even for the highest source rate, the interaction between the directional antenna model with larger beamwidths (e.g., 10 degrees) and the spatial distribution of the MPCs does not result into different throughput or latency for the HB and FS channel models. When smaller beamwidths are used (i.e., 2 degrees), there is instead a difference in performance between the HB and FS models for both source rate values, showing that the modeling of the interaction between the antenna model and the channel model has an impact on the full stack performance.

Finally, we analyze the effect of beamwidth on the received power. In particular, Figure 10 reports the evolution of the received power vs. time, with users following the mobility pattern of Figure 2, for a single simulation run. For this figure, the NLOS/LOS transition

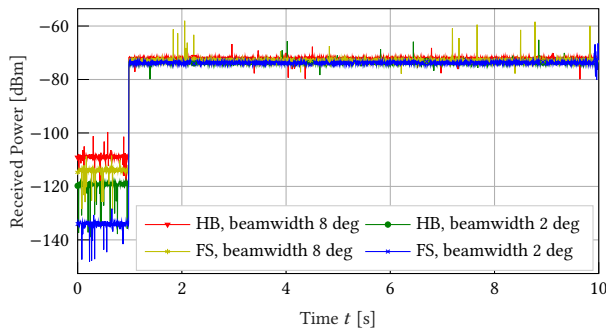


Figure 10: Received power with different channel models and beams.

of the FS channel is not random, but it follows that modeled through the RT for the specific simulation scenario. In NLOS (i.e., before $t = 1.5$ s), there is a significant difference between the different channel models, with an average gap of 10 dB between the two beamwidth values for HB, and of 25 dB for FS. The different beamwidths and channel models have a more limited impact in the LOS scenario, i.e., after $t = 1.5$ s, due to the direct link between RX and TX. The results of Figure 10 also highlight one shortcoming of currently available models for above 100 GHz, i.e., the lack of a temporal characterization of the LOS/NLOS transitions.

5 CONCLUSIONS

This paper introduced the implementation of two SCMs for the ns-3 module TeraSim, based on the 140 GHz models from [5, 12]. This makes it possible to simulate LOS and NLOS scenarios for future 6G networks, including fading and the possibility to interact with antenna array models. We also compared the two channel models (based on a fully stochastic and an RT-based modeling) with simulations in an indoor scenario, which have highlighted how the two modeling strategies differ in their interaction with the directional antenna model of TeraSim.

As future work, we will further expand the analysis of the full-stack performance, including different source traffic patterns, scenarios, and different protocol stack implementations.

ACKNOWLEDGMENTS

This work is supported in part by the EU MSCA ITN project MINTS “Millimeter-wave NeTworking and Sensing for Beyond 5G” (grant no. 861222).

REFERENCES

- [1] 3GPP. 2018. *NR; Overall description; Stage-2*. Technical Specification (TS) 38.300. Version 15.0.0.
- [2] 3GPP. 2021. Study on supporting NR from 52.6 GHz to 71 GHz. TR 38.808, Rel. 17.
- [3] Ian F Akyildiz, Josep Miquel Jornet, and Chong Han. 2014. Terahertz band: Next frontier for wireless communications. *Physical Communication* 12 (Sep 2014), 16–32.
- [4] Georgia E Athanasiadou and Andrew R Nix. 2000. A novel 3-D indoor ray-tracing propagation model: The path generator and evaluation of narrow-band and wide-band predictions. *IEEE Transactions on Vehicular Technology* 49, 4 (July 2000), 1152–1168.
- [5] Yi Chen, Yuanbo Li, Chong Han, Ziming Yu, and Guangjian Wang. 2021. Channel Measurement and Ray-Tracing-Statistical Hybrid Modeling for Low-Terahertz

- Indoor Communications. *IEEE Transactions on Wireless Communications*. Early Access (2021). <https://doi.org/10.1109/TWC.2021.3090781>
- [6] Paul Ferrand, Mustapha Amara, Stefan Valentin, and Maxime Guillaud. 2016. Trends and challenges in wireless channel modeling for evolving radio access. *IEEE Communications Magazine* 54, 7 (July 2016), 93–99.
- [7] M. Giordani, M. Polese, M. Mezzavilla, S. Rangan, and M. Zorzi. 2020. Toward 6G Networks: Use Cases and Technologies. *IEEE Commun. Mag.* 58, 3 (March 2020), 55–61. <https://doi.org/10.1109/MCOM.001.1900411>
- [8] Chong Han, A. Ozan Bicen, and Ian F. Akyildiz. 2015. Multi-Ray Channel Modeling and Wideband Characterization for Wireless Communications in the Terahertz Band. *IEEE Transactions on Wireless Communications* 14, 5 (May 2015), 2402–2412. <https://doi.org/10.1109/TWC.2014.2386335>
- [9] Chong Han and Yi Chen. 2018. Propagation Modeling for Wireless Communications in the Terahertz Band. *IEEE Communications Magazine* 56, 6 (June 2018), 96–101. <https://doi.org/10.1109/MCOM.2018.1700898>
- [10] Zahed Hossain, Qing Xia, and Josep Miquel Jornet. 2018. TeraSim: An ns-3 extension to simulate Terahertz-band communication networks. *Nano Communication Networks* 17 (Sep 2018), 36–44.
- [11] Josep Miquel Jornet and Ian F Akyildiz. 2011. Channel modeling and capacity analysis for electromagnetic wireless nanonetworks in the terahertz band. *IEEE Transactions on Wireless Communications* 10, 10 (Aug 2011), 3211–3221.
- [12] Shihao Ju, Yunchou Xing, Ojas Kanhere, and Theodore S. Rappaport. 2021. Millimeter Wave and Sub-Terahertz Spatial Statistical Channel Model for an Indoor Office Building. *IEEE Journal on Selected Areas in Communications* 39, 6 (Apr 2021), 1561–1575.
- [13] Mattia Lecci, Michele Polese, Chieping Lai, Jian Wang, Camillo Gentile, Nada Golmie, and Michele Zorzi. 2020. Quasi-Deterministic Channel Model for mmWaves: Mathematical Formalization and Validation. In *IEEE Global Communications Conference (GLOBECOM)*.
- [14] Mattia Lecci, Paolo Testolina, Michele Polese, Marco Giordani, and Michele Zorzi. 2021. Accuracy vs. Complexity for mmWave Ray-Tracing: A Full Stack Perspective. *IEEE Transactions on Wireless Communications* (Jun 2021).
- [15] Yuanbo Li, Ning Li, and Chong Han. 2021. Ray-tracing Simulation and Hybrid Channel Modeling for Low-Terahertz UAV Communications. In *IEEE International Conference on Communications (ICC)*. 1–6. <https://doi.org/10.1109/ICC42927.2021.9500549>
- [16] Anamaria Moldovan, Michael A. Ruder, Ian F. Akyildiz, and Wolfgang H. Gerstacker. 2014. LOS and NLOS channel modeling for terahertz wireless communication with scattered rays. In *IEEE Globecom Workshops (GC Wkshps)*. 388–392.
- [17] Bile Peng, Ke Guan, Alexander Kuter, Sebastian Rey, Matthias Patzold, and Thomas Kuerner. 2020. Channel Modeling and System Concepts for Future Terahertz Communications: Getting Ready for Advances Beyond 5G. *IEEE Vehicular Technology Magazine* 15, 2 (June 2020), 136–143. <https://doi.org/10.1109/MVT.2020.2977014>
- [18] Vitaly Petrov, Thomas Kurner, and Iwao Hosako. 2020. IEEE 802.15. 3d: First standardization efforts for sub-terahertz band communications toward 6G. *IEEE Communications Magazine* 58, 11 (Nov 2020), 28–33.
- [19] Radoslaw Piesiewicz, Christian Jansen, S Wietzke, Daniel Mittleman, Martin Koch, and Thomas Kürner. 2007. Properties of building and plastic materials in the THz range. *International Journal of Infrared and Millimeter Waves* 28, 5 (May 2007), 363–371.
- [20] Michele Polese, Josep Miquel Jornet, Tommaso Melodia, and Michele Zorzi. 2020. Toward End-to-End, Full-Stack 6G Terahertz Networks. *IEEE Communications Magazine* 58, 11 (November 2020), 48–54.
- [21] Theodore S. Rappaport, Shu Sun, Rimma Mayzus, Hang Zhao, Yaniv Azar, Kevin Wang, George N. Wong, Jocelyn K. Schulz, Mathew Samimi, and Felix Gutierrez. 2013. Millimeter Wave Mobile Communications for 5G Cellular: It Will Work! *IEEE Access* 1 (May 2013), 335–349.
- [22] Hadi Sarieddeen, Nasir Saeed, Tareq Y. Al-Naffouri, and Mohamed-Slim Alouini. 2020. Next Generation Terahertz Communications: A Rendezvous of Sensing, Imaging, and Localization. *IEEE Communications Magazine* 58, 5 (May 2020), 69–75.
- [23] Priyanshu Sen, Viduneth Ariyaratna, Arjuna Madanayake, and Josep M. Jornet. 2020. Experimental Wireless Testbed for Ultrabroadband Terahertz Networks. In *Proceedings of the 14th International Workshop on Wireless Network Testbeds, Experimental Evaluation & Characterization (WiNTECH'20)*. London, United Kingdom, 48–55.
- [24] Qing Xia, Zahed Hossain, Michael Medley, and Josep Miquel Jornet. 2021. A Link-Layer Synchronization and Medium Access Control Protocol for Terahertz-Band Communication Networks. *IEEE Transactions on Mobile Computing* 20, 1 (Jan 2021), 2–18.
- [25] Menglei Zhang, Michele Polese, Marco Mezzavilla, Jing Zhu, Sundeep Rangan, Shivendra Panwar, and Michele Zorzi. 2019. Will TCP Work in mmWave 5G Cellular Networks? *IEEE Communications Magazine* 57, 1 (January 2019), 65–71.